Electrochemical impedance spectroscopy investigation of the electrochemical behaviour of copper coated with artificial patina layers and submitted to wet and dry cycles

R. del P.B. Hernandez, I.V. Aoki, Bernard Tribollet, Hercilio G. de Melo

Electrochemical impedance spectroscopy investigation of the electrochemical behaviour of copper coated with artificial patina layers and submitted to wet and dry cycles

R. del P.B. Hernández [a], I.V. Aoki [a,1], B. Tribollet [b,1], H.G. de Melo [a,*,1]

[a] *Chemical Engineering Department of the Polytechnic School of the University of São Paulo, P.O. Box 61548, CEP: 05424-970, São Paulo, SP, Brazil*
[b] *LISE, UPR 15 du CNRS, Université Pierre et Marie Curie, Cp 133, 4 Place Jussieu, 75252 Paris Cedex 05, France*

ABSTRACT

Due to rain events historical monuments exposed to the atmosphere are frequently submitted to wet and dry cycles. During drying periods wetness is maintained in some confined regions and the corrosion product layer, generally denominated patinas, builds up and gets thicker. The aim of this study is to use electrochemical impedance spectroscopy (EIS) to investigate the electrochemical behaviour of pure copper coated with two artificial patina layers and submitted either to continuous or to intermittent immersion tests, this latter aiming to simulate wet and dry cycles. The experiments were performed in 0.1 mol dm^{-3} NaCl solution and in artificial rainwater containing the most significant pollutants of the city of São Paulo. The results of the continuous immersion tests in the NaCl solution have shown that the coated samples behave like a porous electrode with finite pore length. On the other hand, in the intermittent tests a porous electrode response with semi-infinite pore length can be developed. The results were interpreted based on the model of de Levie and a critical comparison with previous interpretations reported in the literature for similar systems is presented.

© 2011 Elsevier Ltd. Open access under the Elsevier OA license.

1. Introduction

Long-term atmospheric exposure of metals leads to uneven corrosion processes [1], which extent is mainly dependent on intensity and frequency of rain events, relative humidity, pollutant concentration and its composition in the atmosphere, all these factors being determinant for the formation of the corrosion product layer. The understanding of this type of corrosion is very important for copper and its alloys, particularly bronze, as they are widely used to produce materials permanently exposed to open atmospheres like electronic devices [1] and metallic artefacts [2,3]. It is well documented that the extent of the corrosion process and the composition of the patina layer is widely dependent on the exposure conditions [2,4–6] as species from the close environment can be incorporated mainly on its outermost layer.

Rain events and humidity play a key role in the patina formation. Initially, they can be regarded as the main sources of electrolyte feeding electrochemical reactions; moreover they also leach pollutants from the atmosphere increasing the aggressiveness of the electrolyte. On the other hand, rain events also provide a mechanism to clean the surface from heavily deposited materials occurring during drying periods. According to Zhang et al. [5] the copper patina runoff (chemical dissolution) rate is higher than the corrosion rate during a rain event; however on a yearly time span the former is significantly less than the latter, and this must contributes to patina thickening. Indeed, after rain events the corrosion product layer remains wet feeding the corrosion reaction [3], evaporation leads to increasing ionic concentration and electrochemical activity, under such condition saturation can easily occurs leading to salt precipitation and patina thickening [1].

Copper and bronze artefacts, either due to prolonged exposure to atmosphere or to burial, are frequently coated with a thick patina layer. In the literature it has been frequently reported that patinas formed on these metals have multi-layered structures [5,7–10], which, according to several authors [10–12], can be reproduced by artificial patina production procedures using different methodologies and electrolytes. This is very useful for investigation of the electrochemical behaviour of copper and bronze artefacts coated with thick corrosion product layers, as, due to the uniqueness of each piece, generally, it is not allowed to modify or damage them even for scientific investigation [10]. According to Rosales [13] the increasing pollution levels in today's world predicts the necessity of controlling the patination process that was formerly left to the action of nature, demonstrating that artificial patinas production is also important for the recovery of damaged areas of artefacts.

Electrochemical impedance spectroscopy (EIS) is a unique technique for following the electrochemical behaviour of metals exposed to different electrolyte. As perturbation of low amplitude

---

* Corresponding author. Tel.: +55 1130912231; fax: +55 1130313020.
E-mail address: hgdemelo@usp.br (H.G. de Melo).
[1] Active ISE members.

Table 1
Composition of the solutions used to produce the patinas [14].

Solutions composition	Nitrates (g dm^{-3})		Chlorides (g dm^{-3})		Oxidizing agent (vol%)
S1	Cu(NO$_3$)$_2$	85	FeCl$_3$,		H$_2$O$_2$,
	ZnNO$_3$	85	3		3
S2	Cu(NO$_3$)$_2$	200	ZnCl$_2$, 200		–

is employed, the electrode is hardly deviated from the stationary conditions and it is not damaged during the experiments. The aim of this work is to use EIS to investigate the electrochemical behaviour of copper electrodes coated with two different types of artificial patinas and exposed either to 0.1 mol dm^{-3} NaCl solution or to synthetic rainwater of São Paulo. Experiments were performed under continuous or intermittent exposure conditions.

2. Experimental

Round-shaped pure copper (99.99%) coupons (2.1 cm^2 of exposed area) were used as working electrode (WE). After being provided with electrical contact, they were embedded by hot resin mounting and sequentially ground with silicon carbide emery paper up to 600 grit, then rinsed with deionized water and alcohol and dried under hot air stream.

The patinas were produced by dabbing the surface of the WEs with a cotton swab soaked with solution S1 or S2 twice a day for five consecutive days, following recipes previously used by Costa and Texier [14]. Between each application the WEs were left to dry at open air at the laboratory atmosphere. This was followed by supplementary 24 h exposure after the last application to allow for drying of the patinas. Table 1 presents the compositions of the two solutions used to produce the artificial patinas. For the sake of simplicity, throughout this work, the patinas will be denominated in accordance with the solution used to produce them: S1 or S2.
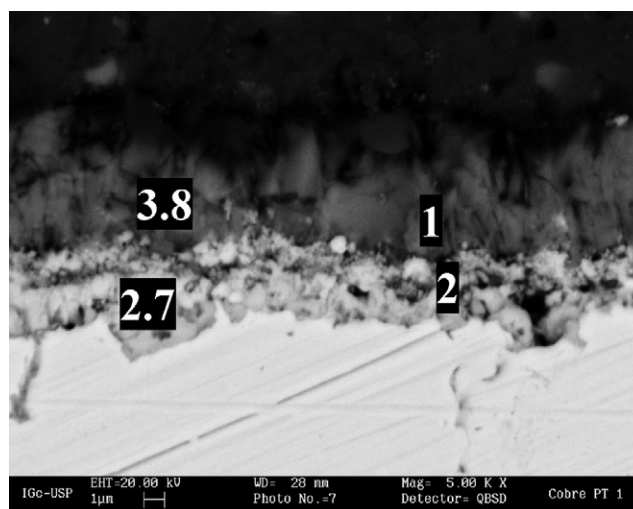
The test solutions were NaCl 0.1 mol dm^{-3} and synthetic rainwater of São Paulo, which composition, given in Table 2, was based on the work of Leal et al. [15].

The electrochemical tests were performed using a conventional three-electrode cell arrangement, with Ag/AgCl(KCl sat.) and a platinum grid as reference and auxiliary electrode, respectively. The tests were carried out using a Sl 1287 electrochemical interface coupled to a Sl 1260 Frequency Response Analyzer both connected to a PC and piloted by the Corrware® software. The EIS diagrams were obtained in potentiostatic mode at the open circuit potential, OCP, with ac perturbation amplitude of 15 mV (rms) in the frequency range from 100 or 10 kHz to 10 mHz, with 10 points per logarithm decade.
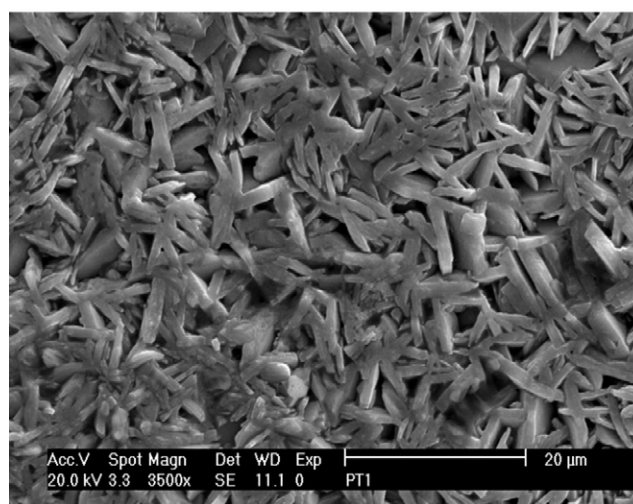
The EIS response of the patina coated samples was evaluated through two different tests: in the first one, denominated continuous immersion tests, the sample remained totally immersed in the test electrolyte throughout the whole experiment (total duration of approximately 3 days), and in the other, intermittent immersion tests, the sample remained immersed in the solution only during the time necessary to acquire the experimental data (approximately 1 h: half an hour for OCP stabilization and half an hour for EIS data acquisition). In this latter test the samples were exposed to the laboratory atmosphere between successive experiments and EIS diagrams were acquired after 1, 7, 14, 28 and 56

Table 2
Composition of the synthetic rainwater of São Paulo [15].

	Compounds (μg dm^{-3})					
	NaNO$_2$	NaNO$_3$	(NH$_4$)$_2$·SO$_4$	(COONH$_4$)$_2$·H$_2$O	(NH$_4$)Cl	pH
São Paulo	41	2764	2405	122	894	4.99

(a)

(b)

Fig. 1. SEM images of the cross-section (5000×) (a) and of the surface (3500×) (b) of a copper sample coated with patina S1. In (a) the thicknesses (μm) of the layers are indicated.

days of patina preparation. These tests were conceived in order to simulate wet/dry cycles.
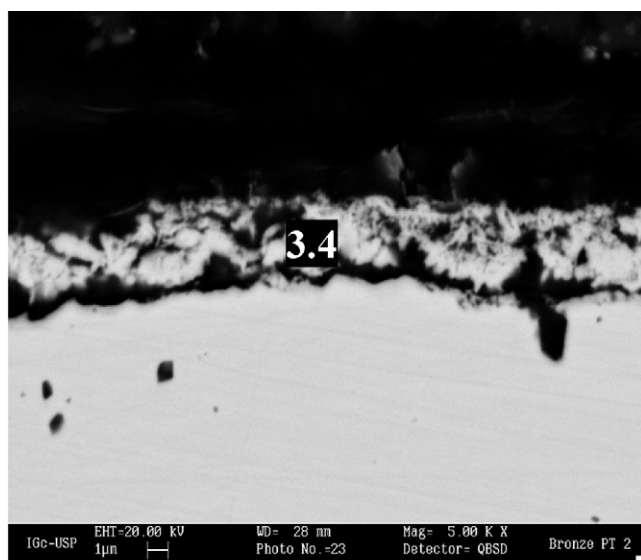
Scanning electron microscopy (SEM-EDS) characterization was performed in the secondary electrons mode (20 keV) using a Philips XL30 equipment. Top and cross-sectional views were observed, for this latter observation the samples were polished with diamond paste until mirror finishing.

The patinas chemical compositions were determined through X-ray diffraction (XRD) with a Philips diffractometer equipped with a copper anticathode (λ = 1.5406 Å). Sweeping was made between 10 and 90° with steps of 0.005. Peaks identification was performed by comparing with Joint Committee on Powder Diffraction Standards (JCPDS) files.
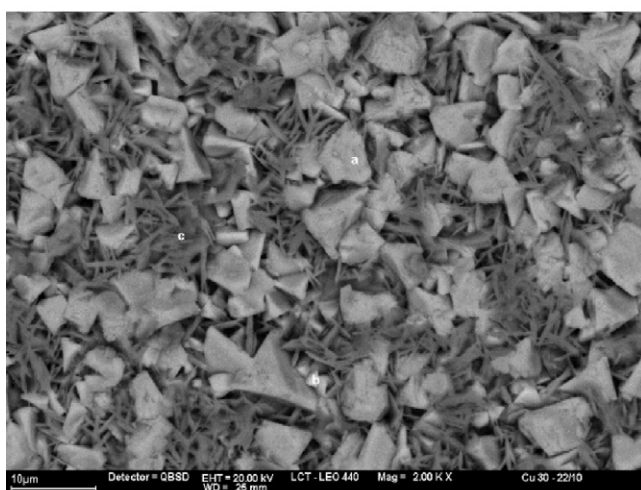
3. Results

3.1. SEM-EDS characterization

Fig. 1(a) and (b) presents, respectively, the cross-section and the top view of a copper sample coated with the patina S1. This patina presents a porous bi-layer structure with a total thickness of
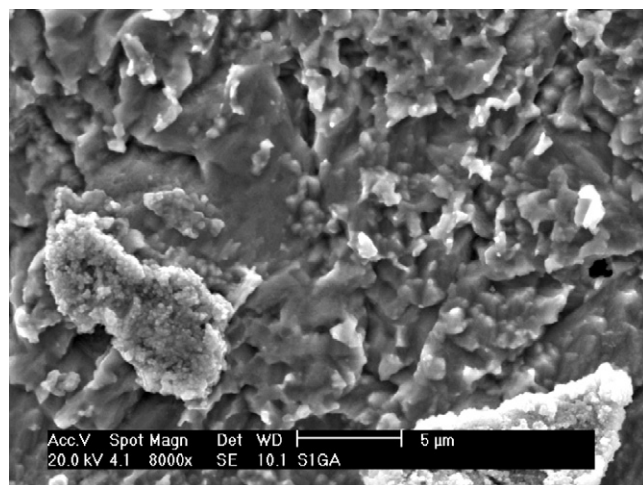
(a)

(b)

Fig. 2. SEM images of the cross-section (5000×) (a) and of the surface (2000×) (b) of a copper sample coated with patina S2. In (a) the thickness (μm) of the layer is indicated.

Fig. 3. SEM image of the surface of a copper sample coated with patina S1 after removal of the patina layer in ultrasonic bath.

the layer and the substrate was verified during embedment procedures performed for cross-section observations, as depicted in Fig. 1(a).

The adherence of the patinas to the copper substrate was evaluated by immersion of patinated samples in water and sonication during 15 min. Even though this treatment did not resulted in the removal of the entire patina layer, both patina S1 and S2 were detached in some regions exposing the underlying substrate. Fig. 3 presents a SEM image of a copper sample coated with the S1 patina after the sonication treatment. It shows that the underlying substrate is very rough, which must be resultant of the extreme etching of the surface by the patina solution during the production procedure. Although not shown here, copper samples coated with the S2 patina presented a similar appearance in regions where the patina was detached; however the detached area was larger for this patina, in accordance with its apparent lower adherence to the substrate (Fig. 2(a)).
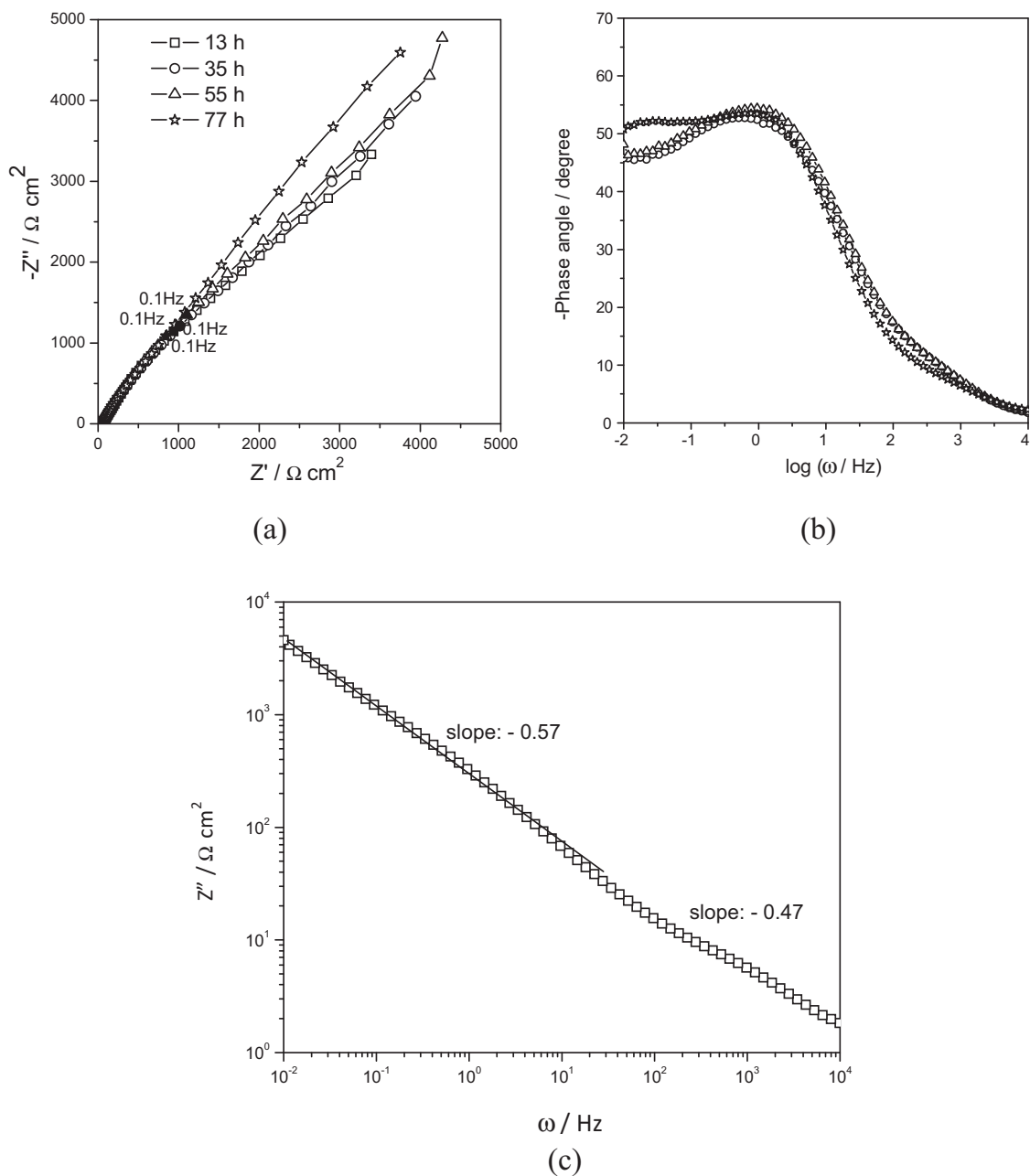
3.2. Electrochemical investigation

3.2.1. Continuous immersion tests

During the immersion tests in the two solutions the general appearance of the samples were frequently observed in order to confirm the integrity of the patinas on their surfaces. It was verified that the S2 patina was dissolved after few hours of immersion in the São Paulo synthetic rainwater solution, for this reason the electrochemical behaviour of this patina was not investigated in this particular solution.

Impedance diagrams after different times for copper samples coated with patina S1 or S2 and continuously immersed in the 0.1 mol dm^{-3} NaCl solution are presented, respectively, in Figs. 4 and 5. In both cases, the diagrams show little evolution with immersion time, indicating that the corrosion products formed are not protective, even though the impedance modulus exhibited by the sample coated with patina S1 was higher. This issue can be related to the superior thickness of the patina layer on this latter sample, as it is known that the transport of species through a porous layer is inversely proportional to its thickness. Even though only one time constant is clearly distinguished in the Nyquist diagrams; the analysis of the Bode phase angle diagrams indicates the existence of two poorly resolved relaxation phenomena, this feature being particularly evident for the S2 patina (Fig. 5).

Figs. 4(c), 5(c) and 5(d) show the plots of the logarithm of the imaginary part of the impedance against the logarithm of the fre-

about 6.5 μm, and the surface is uniformly covered with needle-like crystals. EDS analyses performed on the top layer showed intense peaks of Cu, N and O, while in the internal layer only Cu and Cl peaks were predominantly identified [16]. These peaks have close relation with the patina solution composition and point towards the combination between copper ions and the anions in solution.

Fig. 2(a) and (b) presents, respectively, the cross-section and the top view of the patina obtained with solution S2. This patina presents a porous monolayer structure, with a thickness of about 3.4 μm, where two different crystalline phases coexist. EDS analyses performed on the two different regions of Fig. 2(b) showed that the needle-like crystals are rich in Cu and N, while the geometric ones present peaks of Cu, Zn and Cl. [16]. The comparison of the cross-section micrographs presented in Figs. 1(a) and 2(a) shows that the thickness of the S1 patina is approximately two times higher than the S2, indicating, that the solution used to produce the former patina is more oxidant than that used to produce the latter. Moreover adherence to the substrate seems to be superior for patinas produced with the S1 formulation as no detachment between
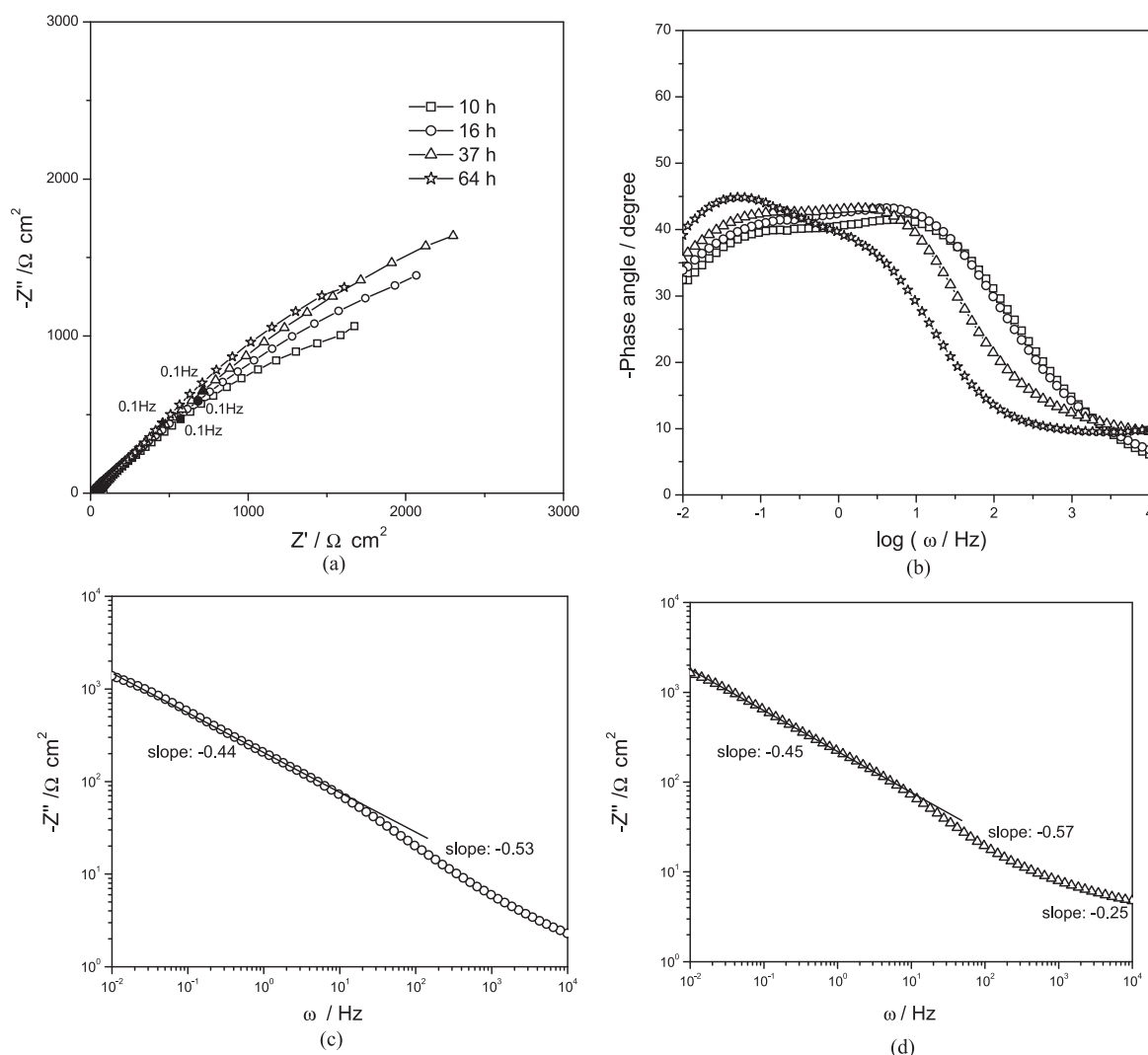
Fig. 4. Impedance diagrams: Nyquist (a) and Bode phase angle (b) plots for copper samples coated with S1 patina and continuously immersed in 0.1 mol dm^{-3} NaCl solution. Plot of the logarithm of the imaginary part of the impedance against the logarithm of the frequency for the diagram obtained after 77 h of immersion (c). In (c) the slopes associated to each linear region are presented.

quency for selected EIS diagrams acquired for samples coated with patina S1 or S2. This representation permits to get rid of the influence of the electrolyte resistance on the high frequency (HF) region of the diagrams and allows directly extracting the exponent of the constant phase element (CPE) when the impedance behaviour deviates from purely capacitive [17]. The figures clearly show the existence of two time constants in the investigated frequency domain, characterized by two straight lines, Figs. 4(c) and 5(c), the lower frequency ones are evidenced by superposing a full line. For all diagrams, the slopes of the straight lines, indicated in the figures, are close to 0.5, these values would represent the exponent of the CPE associated with each time constant [17], and their meaning will be discussed later. For the diagram depicted in Fig. 5(d) a third time constant is detected at the highest frequency limit indicating the existence of a new impedance sensitive phenomenon, this par-

ticular time constant points to a very depressed capacitive loop and the slope of the straight line is very close to 0.25.

Fig. 6(a) depicts the impedance response of copper samples coated with patina S1 and continuously immersed in the São Paulo synthetic rainwater solution. Due to the lower aggressiveness of this medium impedances were clearly superior to those obtained in the 0.1 mol dm^{-3} NaCl solution. Moreover, the impedance increases up to 48 h of immersion and then remains almost constant, indicating the build-up of protective corrosion products. For short immersion periods two capacitive time constants are distinguishable in the diagrams, however the HF one vanishes after longer test periods. Fig. 6(b) presents a comparison between the impedance responses of a pure copper sample and a sample coated with the S1 layer after about 72 h of immersion in the synthetic rainwater of São Paulo. The phase angles and the Nyquist diagrams are very

Fig. 5. Impedance diagrams: Nyquist (a) and Bode phase angle (b) plots for copper samples coated with S2 patina and continuously immersed in 0.1 mol dm^{-3} NaCl solution. Plot of the logarithm of the imaginary part of the impedance against the logarithm of the frequency for the diagrams obtained after 16 h (c) and 37 h (d), with the slopes associated to each linear region.

similar in shape indicating that the patina S1 does not afford any additional corrosion protection to the copper substrate, and that the same corrosion process must takes place in both samples.

3.2.2. Intermittent immersion tests

The impedance diagrams obtained during the intermittent immersion tests performed with copper coated with patina S1 in 0.1 mol dm^{-3} NaCl solution are shown in Fig. 7. After one day of patina production, the impedance response is low, demonstrating high surface activity, which is indicative that the oxidizing patina solution continues to attack the copper surface. On the other hand, for the tests performed after 7, 15 and 28 days of patina production almost no change was verified in the impedance modulus, which is of the same order of magnitude to that obtained in the continuous immersion tests (Fig. 4). However, as shown in Fig. 7(c), after 28 days of patina production (corresponding to four immersion periods) a HF capacitive loop starts to develop indicating the onset of a new impedance sensitive phenomenon. This flattened loop is completely developed after 56 days of patina production (5 immersion periods), Fig. 7(d), and is associated with an important increase in the impedance response, indicating better anticorrosion performance, this evolution is accompanied by diffusion-like LF response. It is well

known from the literature that wetting-drying periods lead to increased patina thicknesses [2,3,13], during drying period drastic changes must occur in the composition of the solution entrapped within the patina layer. Nassau et al. [18] have shown that water evaporation leads to pH decreasing provoking an increase in the corrosion rate, on the other hand, copper corrosion reactions increase the pH favouring precipitation reactions. The balance between these two opposing tendencies must govern the precipitation of the corrosion products and the consolidation of the patina layer, increasing its thickness and improving its protective properties.

For the copper sample treated with the patina S2 the impedance responses for the intermittent experiments are presented in Fig. 8. The results were qualitatively very similar to those obtained with the sample coated with the S1 patina, *i.e.*, after 28 days of test (corresponding to 4 immersion periods), a flattened HF loop starts to build up, which is completely developed after 56 days of test (5 immersion periods), when a diffusion-like LF response is perceptible. The only noticeable difference between the two set of experiments is that, for patina S2, a constant increase of impedance was verified for increasing immersion time. In addition, Figs. 7 and 8 also show that at the end of the testing period (56 days) the impedances of the copper samples coated with both patinas are of the same order
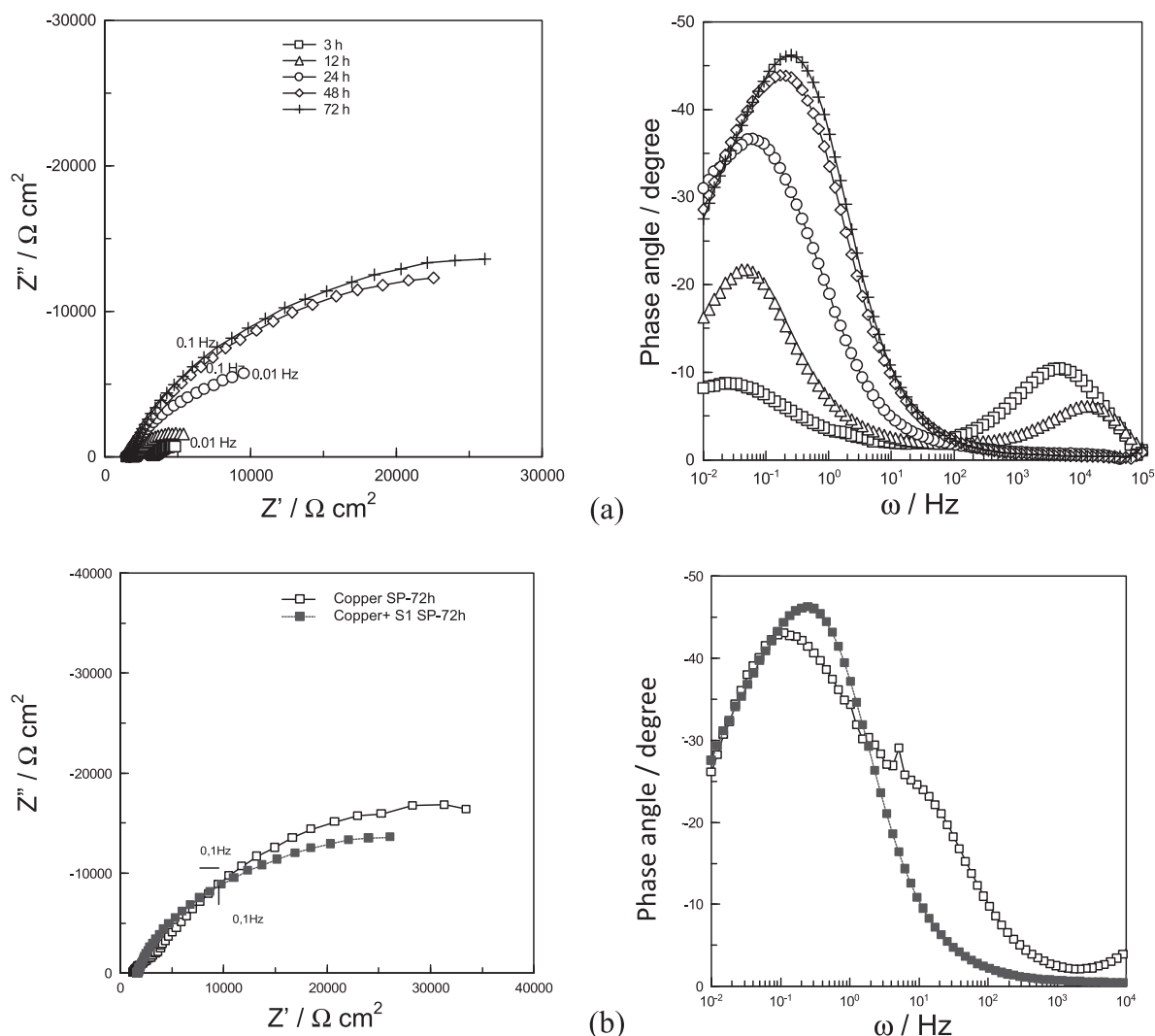
Fig. 6. Impedance diagrams for copper samples coated with S1 patina and continuously immersed in synthetic rainwater of São Paulo (a). Comparison between the impedance response of pure copper and copper coated with S1 patina after about 72 h in the same solution (b).

of magnitude indicating similar protective properties, even though, after production, patina S2 has half of the thickness of the S1.

The results of the intermittent tests carried out with the copper sample coated with patina S1 in the São Paulo synthetic rainwater are shown in Fig. 9. The tests were performed until 28 days, corresponding to 4 immersion periods. For this particular solution the flattened HF loop is already evident after 15 days of patina production (corresponding to 3 immersion periods), which becomes even more depressed after 28 days of test (4 immersion periods). For this particular sample the LF capacitive loop also becomes fairly flattened in the last experiment of the series.

4. Discussion

For the series of experiments presented in Figs. 4 and 5 flattened capacitive loops were obtained in the Nyquist plots, which are resultant from two poorly resolved relaxation phenomena, as seen in the Bode phase angle plots. These diagrams are qualitatively very similar to those reported by Deslouis et al. [20] for a copper electrode in neutral 0.5 mol dm^{-3} NaCl solution, indicating that a similar corrosion mechanism must takes place. Based on steady state measurements and impedance calculations these authors [19,20] have proposed that in such solution copper corrosion proceeds through the sequence of steps presented in Eqs. (1) and (2). They have ascribed the LF response of the EIS diagrams to a mass transport controlled process limited by the diffusion of the copper chloride complex (CuCl$_2^-$) both in the solution and through a porous layer of corrosion product [20], which, in the present case, must also include the patina layer. This latter feature can explain the higher impedance values obtained for the sample coated with the patina S1 since it is thicker than patina S2. On the other hand, the flattened appearance of the HF loop was attributed by Deslouis et al. to time constant dispersion phenomena [20]:

$$Cu + Cl^- \leftrightarrow CuCl + e^- \tag{1}$$

$$CuCl + Cl^- \leftrightarrow CuCl_2^- \tag{2}$$
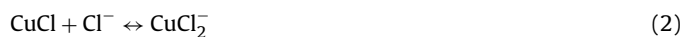
The plots of the imaginary part of the impedance against the logarithm of the frequency (Figs. 4(c) and 5(c)), which gives the CPE exponents values [17], show that the slopes of the straight lines are very close to 0.5 for all the time constants. While the exponent of the LF time constant is coherent with a mass transport controlled process as proposed by Deslouis et al. [19,20], the HF behaviour seems to indicate the response of a porous electrode as predicted by the de Levie's theory [21,22]. According to this theory the impedance
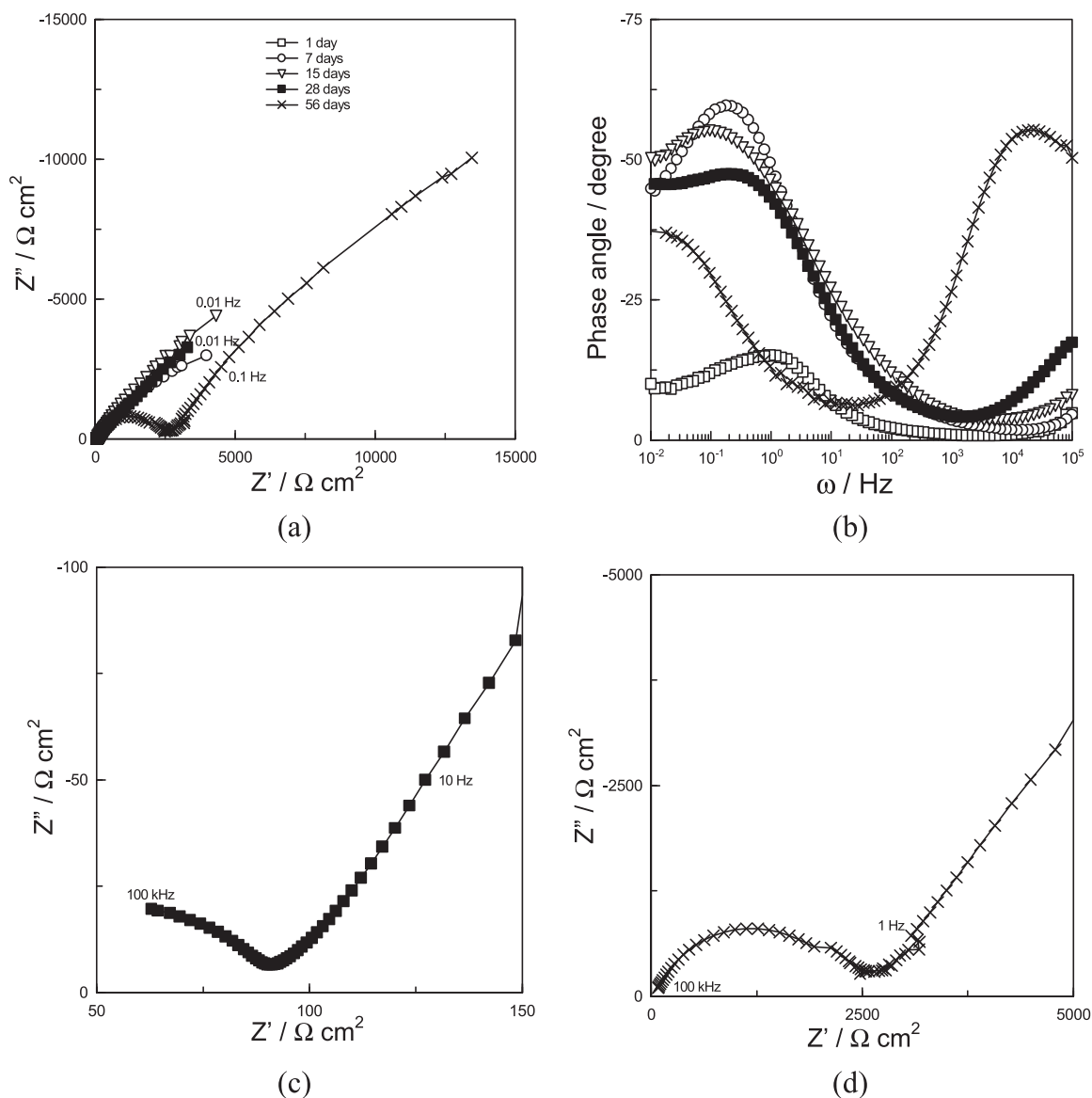
Fig. 7. Impedance diagrams for copper samples coated with S1 patina submitted to intermittent immersion tests in 0.1 mol dm^{-3} NaCl solution: Nyquist (a) and Bode phase angle (b) plots. Detail of the high frequency region of the Nyquist diagrams for patinas produced after 28 days (c) and 56 days (d). Impedance after 1 day is too low and not visible in Nyquist diagrams.

of a cylindrical pore is given by the following relation [23]:

$$Z_P = \sqrt{R_C Z_0} \coth\left(\frac{l_C}{\lambda}\right) \text{ with } \lambda = \sqrt{\frac{Z_0}{R_C}} \tag{3}$$

where Z_P corresponds to the impedance of the cylindrical pore (Ω), R_C is the resistance of the electrolyte per unit length within the pore (Ω cm^{-1}), Z_0 is the impedance, per unit length, of the flat electrode developed in the cylindrical pore (Ω cm), l_C is the pore depth (cm) and λ corresponds to the penetration depth of the ac signal in the pore (cm). According to de Levie [21], λ corresponds to the fraction of the pore that effectively participates in the charging process. When $l_C \gg \lambda$ (coth (l_C/λ) $\cong 1$), the impedance of the pore is proportional to the square root of the impedance of the flat electrode, which is the typical response of a porous electrode with semi-infinite pore length [24]. On the other hand, when $l_C/\lambda \leq 0.3$ (coth(l_C/λ) $\cong \lambda/l_C$), the pore is shallow and the impedance is given by relation (4) [25], which is similar to the response exhibited by a

flat electrode:

$$Z_P = \frac{Z_0}{l_C} \tag{4}$$

Even though based on a series of simplifying assumptions the porous electrode model has been successfully employed to explain the EIS behaviour of different electrochemical interfaces [26,27]. Recently Song et al. [28] have shown that porous electrode response depends on pore size distribution, and that the shallower the pore the higher the frequency at which the EIS response deviates from that expected from a porous electrode approaching to that exhibited by a flat one. This indicates that porous and flat electrode responses can co-exist in the same EIS diagram.

Studies performed by Diard et al. [29] and by Matos et al. [30] of copper electrodissolution in 1 mol dm^{-3} HCl solution have shown that the HF capacitive loop of the EIS diagrams makes an angle of approximately 45° with the real axis, while in the LF region the usual mass transport control predicted by Deslouis et al. [19,20] was observed. Matos et al. [30] have interpreted their HF result as
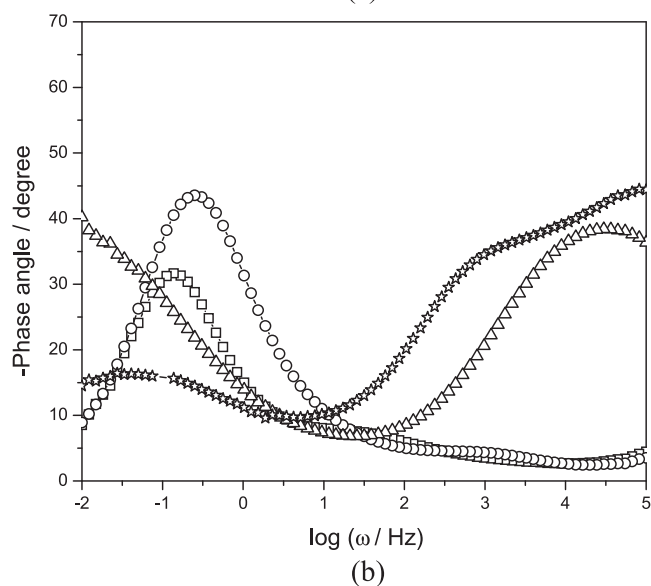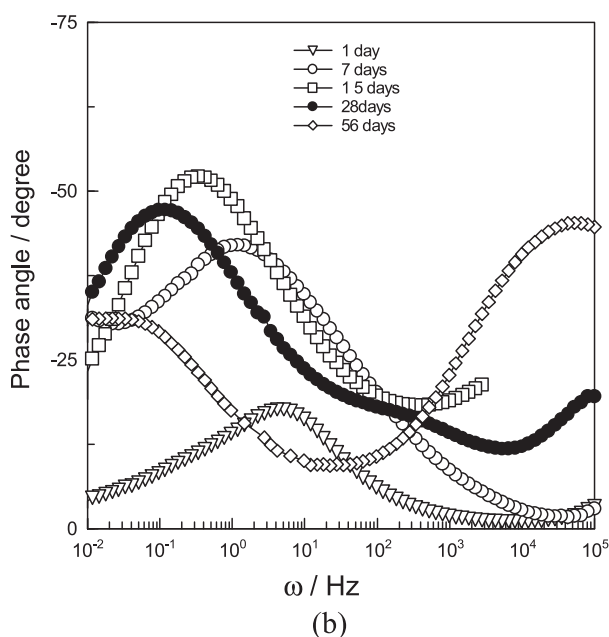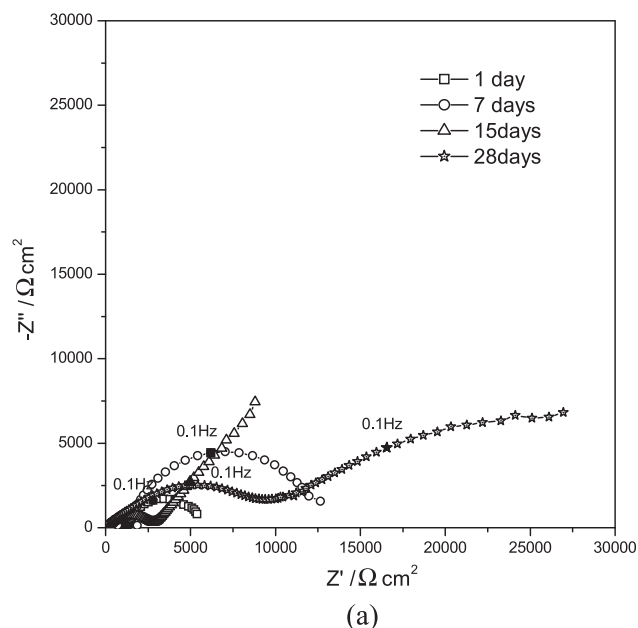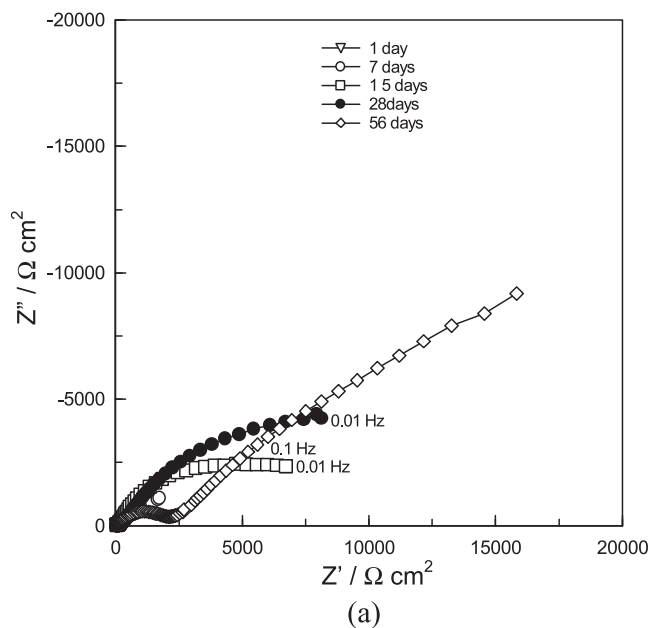
Fig. 8. Impedance diagrams for copper samples coated with S2 patina submitted to intermittent immersion tests in 0.1 mol dm^{-3} NaCl solution: Nyquist (a) and Bode phase angle (b) plots. Impedance after 1 day is too low and not visible in Nyquist diagrams.

Fig. 9. Impedance diagrams for copper samples coated with S1 patina submitted to intermittent immersion tests in synthetic rainwater of São Paulo: Nyquist (a) and Bode phase angle (b) plots.

being due to the response of a porous electrode with finite pore length. In this way, in the HF region, when the penetration depth of the electrical signal is low, the pores behave as if they were semi-infinite and a porous electrode response is obtained; on the other hand, as frequency goes down the penetration depth increases and a flat electrode response is observed. Mixed porous-flat electrode response in the same impedance spectrum has also been found by other authors for other corroding systems [31,32]. Taking into account these interpretations and the rough nature of the substrate (Fig. 3), it is proposed that the patina coated copper samples behave as porous electrodes with finite pore length, and that they corrode similarly to pure copper in acidic chloride solutions, the pores would be developed from the surface roughness as shown in Fig. 3. Moreover, the interpretation of the results indicate that the EIS experiments do not detect the presence of the patinas, even though

they were clearly detectable by the observation of the electrodes surface at naked eye.

The diagram of the imaginary impedance depicted in Fig. 5(d) for the sample coated with the patina S2 after 37 h of immersion in NaCl 0.1 mol dm^{-3} shows the onset of a third time constant in the highest frequency region, characterized by a straight line with slope close to 0.25, which was not observed for the samples coated with the patina S1. In a recent work Gourbeyre et al. [33], investigating the corrosion behaviour of duplex coatings, proposed a model where smaller pores, denominated by the authors as secondary pores, develop in the walls of the main pores of a porous electrode. The EIS response of these smaller pores would be the square root of the impedance of a porous electrode, as predicted by de Levie porous electrode model [21,22], and can likely explain the observed HF behaviour presented for the S2 coated sample after longer immersion periods in the NaCl 0.1 mol dm^{-3} solution. This assumption is even more likely as, like the copper samples after the patina application procedure, the substrate employed by Gourbeyre et al. [33]

presented a rough configuration. The development of the secondary pores and also the fact that the transition between the porous and flat electrode response takes place at lower frequencies for the samples coated with the patina S2 (compare Figs. 4(c) and 5(c)) indicate that pores are deeper in this particular sample if compared to that coated with the S1 patina.

The diagrams presented in Fig. 6 for copper samples coated with S1 patina and continuously immersed in the synthetic rainwater of São Paulo show, for short immersion times, two clearly distinguishable time constants in the Bode phase angle diagrams. We have calculated the capacity associated with the patina S1 using the following relation:

$$C = \frac{\varepsilon\varepsilon^0}{d}A \tag{5}$$

where ε^0 is 8.85×10^{-14} F cm^{-1} (vacuum permittivity), d is the layer thickness (6.5 μm, cf. Fig. 1) and A is the exposed area (2.1 cm^2). For the dielectric constant of the patina layer (ε) we have adopted 80, which corresponds to a completely water-soaked patina layer [34], an assumption compatible with its porous structure and non-protective nature. The substitution of these values in (5) gives a capacity of 2.29×10^{-2} μF. For 3 h of test, corresponding to one of the diagrams where the HF capacitive loop is present in Fig. 6(a), we have also calculated the capacity associated with the HF loop using its characteristic frequency, which is about 3.2 kHz at the loop apex, and a loop diameter of about 1.5 kΩ. This gave a capacity value of 3.31×10^{-2} μF, which is fairly similar to the one calculated using Eq. (5). This indicates that the HF loop, detected in the EIS diagrams for short immersion times, can be ascribed to the patina layer, which is subsequently partially dissolved leading to the loop disappearance. Complete dissolution of the patina layer was ruled out as it was visible by the observation of the WE surface by naked eye until the end of the experiment.

The diagrams presented in Fig. 6(a) show that impedance of the copper sample coated with the S1 patina and immersed in the São Paulo rainwater solution increases with time, additionally their values are clearly superior to those obtained in the 0.1 mol dm^{-3} NaCl solution, demonstrating a lower aggressiveness of the former electrolyte towards copper and the build-up of a protective corrosion product layer. The comparison of the EIS responses of pure copper with that of a sample coated with the S1 patina after around 3 days of immersion in the São Paulo rainwater solution (Fig. 6(b)) shows almost the same behaviour, indicating that the patina does not afford additional anticorrosion protection to the substrate. However, the Bode phase angle diagrams presented in Fig. 6(b) show a HF shoulder for the non-patinated copper sample, which is absent from the diagram of the S1 coated sample. In a recent work Hernández et al. [35] verified that immersion of copper samples in synthetic rainwater of São Paulo for up to three days led to an improvement of the corrosion resistance of the metal. This effect was ascribed to the thickening and healing of the oxide layer (cuprite) associated with the presence of NH$_4^+$ ions. Feng et al. [36], studying the corrosion behaviour of copper in tap water using EIS, determined that at pH 5 (similar to that presented by the synthetic rainwater of São Paulo) mixed diffusion of copper ions both in the solution and within the oxide film controlled the overall corrosion rate. Therefore, it is likely that the HF shoulder observed in the diagram for the copper sample could be ascribed to the presence of a thin oxide (cuprite) layer while the LF region would represent the response of the diffusion controlled processes. Regarding the EIS response of the S1 coated sample, the absence of the HF shoulder would be justified by the etching of the copper substrate during the treatment with the patina solution leading to the formation of an even thinner oxide layer, which, taking into account the EIS results, is not less protective than that present on the surface of non-patinated copper samples.

The EIS diagrams obtained in the 0.1 mol dm^{-3} NaCl solution for copper coated with the S1 patina and submitted to drying periods at the laboratory atmosphere between consecutive tests (Fig. 7) show that, up to 15 days (3 immersion periods), they have similar shapes, and impedance values are of the same order of magnitude to that presented in Fig. 4, indicating that the corrosion mechanism is the same, i.e., the substrate behaves as a porous electrode with finite pore length and dissolution takes place within the pores. However, after 28 days and 56 days of drying, 4 and 5 immersion periods, respectively (Fig. 7(c) and (d)) a depressed HF capacitive loop is developed, demonstrating that a new impedance sensitive process is occurring. As already stated, this is accompanied by an important increase of the impedance, which indicates that this new time constant is associated with a process that affords corrosion protection to the substrate. As shown in Fig. 10(a), the HF region of this new loop is a straight line, which slope is close to 1, indicating that this new process takes place within the pores. We propose that this HF loop is due to the development of a protective corrosion product layer on the pore walls, which precipitates during prolonged drying periods; corrosion activity would take place through the resistive pathways (pores) of this isolating protective layer, and this would correspond to the LF depressed loop. The resemblance of this latter loop with the overall EIS response in the continuous immersion tests (Fig. 4) indicates that the same corrosion mechanism is taking place.

The diagrams acquired during the intermittent tests performed in the NaCl 0.1 mol dm^{-3} solution for copper coated with the S2 patina (Fig. 8) exhibit an evolution similar to that presented in Fig. 7; therefore the same sequence of events must takes place leading to an improvement of the corrosion resistance of the sample. Nevertheless the diagram depicted in Fig. 10(b) shows that the HF capacitive loop is more depressed than that presented in Fig. 10(a), being the angle with the real axis smaller than 45° (the slope of the straight line is lower than 1). The continuous experiments performed with samples coated with the S2 patina showed a particular HF feature (Fig. 5(d)) ascribed to the formation of smaller secondary pores within the main ones in accordance with previous interpretation provided by Gourbeyre et al. [33]; hence the precipitation of the corrosion product layer also inside these pores would explain the increased depression of the HF loop, as the EIS response would also reflect impedance sensitive processes taking place within them. As with patina S1, the resemblance of the LF region with the overall EIS response in the continuous tests (Fig. 5) indicates that the same corrosion process is taking place.

The comparison of Fig. 10(a) and (b) also shows that the LF capacitive loop is more depressed in the intermittent tests performed with the sample coated with the S2 patina. This indicates that deeper pores are formed in this latter sample and a contribution of the porous electrode response would be more effectively detected in the LF loop. This is also in accordance with the findings of the continuous immersion tests where the transition frequency from porous to flat electrode behaviour was found to occur at lower frequencies with the S2 coated samples.

The impedance responses obtained in the intermittent immersion tests in the NaCl 0.1 mol dm^{-3} solution (Figs. 7 and 8) show a continuous increase of the impedance when the copper sample is coated with the patina S2, while when it is coated with the patina S1 a noticeable increase in the impedance was verified only between the fourth (28 days) and the fifth (56 days) immersion period, after the sample has remained approximately 28 days exposed to the laboratory atmosphere. This distinction in the electrochemical behaviour can be related to the differences in the patinas compositions. In experiments dating back to 1922 and aiming to investigate
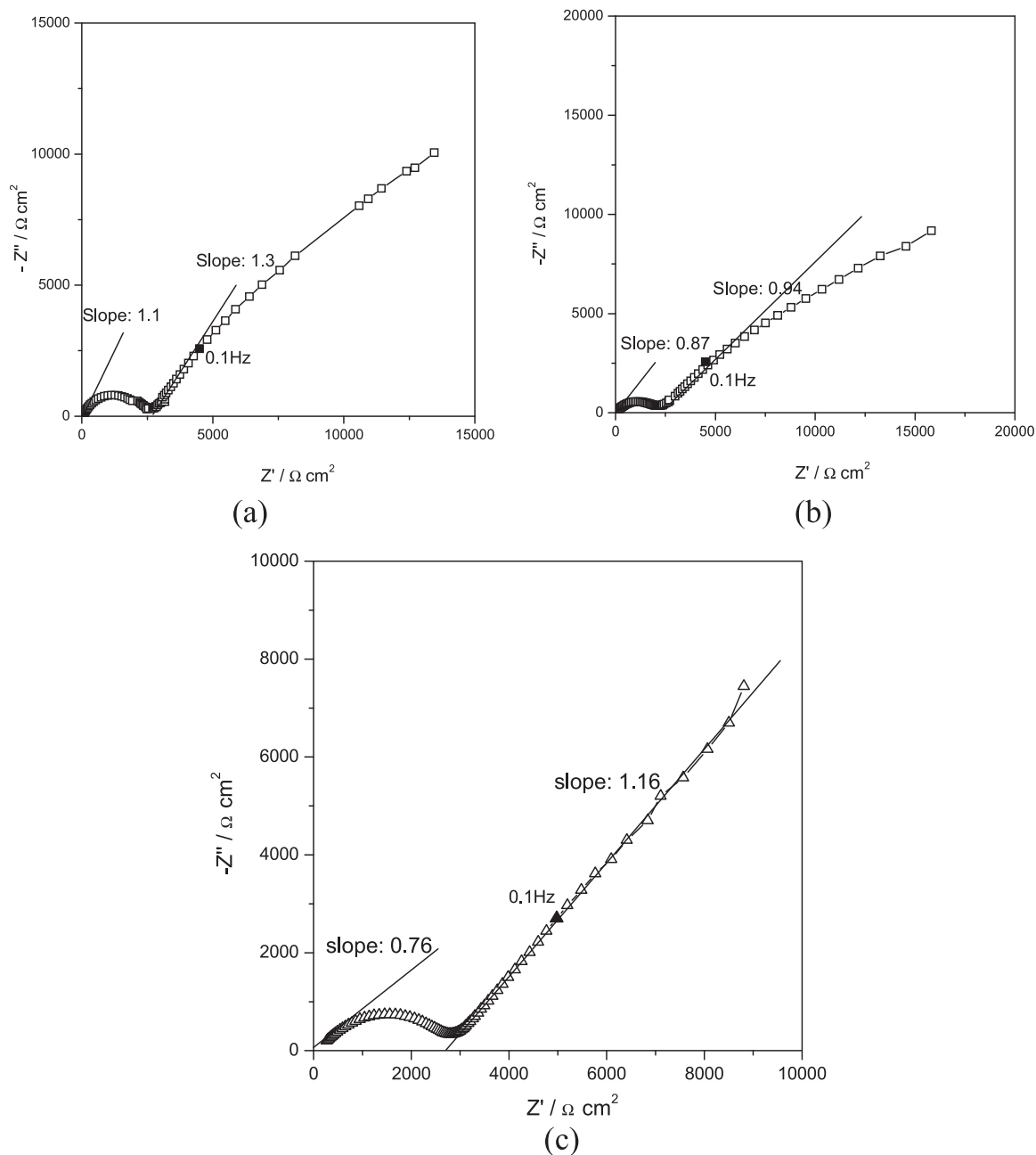
Fig. 10. Nyquist diagrams acquired under intermittent exposure conditions for copper electrodes coated with patinas: (a) S1–5 periods in NaCl 0.1 mol dm^{-3} (56 days); (b) S2–5 periods in NaCl 0.1 mol dm^{-3} (56 days); (c) S1–3 periods in São Paulo synthetic rainwater (15 days). In all the diagrams the slopes of the straight lines between the capacitive loops and the real axis are represented.

the "*dry corrosion*" mechanism of metals, Evans [37] verified that if the main corrosion product is a deliquescent substance, the actual thickness of the moisture-film should notably increase as corrosion proceeds, and corrosion should be accelerated. The author states [37] that, for metal exposed to air, the possibility of the formation of hygroscopic corrosion product is the most important factor in determining the corrosion rate. Therefore, under atmospheric exposure conditions the presence of such substances increases the thickness of the moisture film and the time of wetness feeding the corrosion process. Fig. 11 presents the XRD spectra obtained on copper samples coated with patinas S1 (Fig. 11(a)) and S2 (Fig. 11(b)). For the S1 patina the predominant species are cuprite (Cu_2O) and the copper nitrate gerhardite ($Cu_2NO_3(OH)_3$), probably from the top layer, with some contribution of nantokite (CuCl), which must be present at the bottom layer. On the other

hand, the S2 patina is predominantly composed of cuprite and nantokite with some contributions of gerhardite ($Cu_2NO_3(OH)_3$) and the basic copper chloride atacamite ($Cu_2Cl(OH)_3$). While nantokite, the main component of S2 patina, is almost insoluble in water, gerhardite, the main component of S1 patina, is classified as hygroscopic and deliquescent. Therefore, during exposure to the laboratory atmosphere, for the S1 patina, it is likely that drying process would be slower due to higher copper nitrate content in its structure, increasing the time of wetness and sustaining the corrosion process all over the surface for longer periods. Regarding the composition of patina S2, although basic copper chlorides (which are hygroscopic) and nitrates are also present in its microstructure, the insoluble nantokite is the main component, which must have resulted in faster drying process when this particular formulation was exposed to the laboratory atmosphere in-between
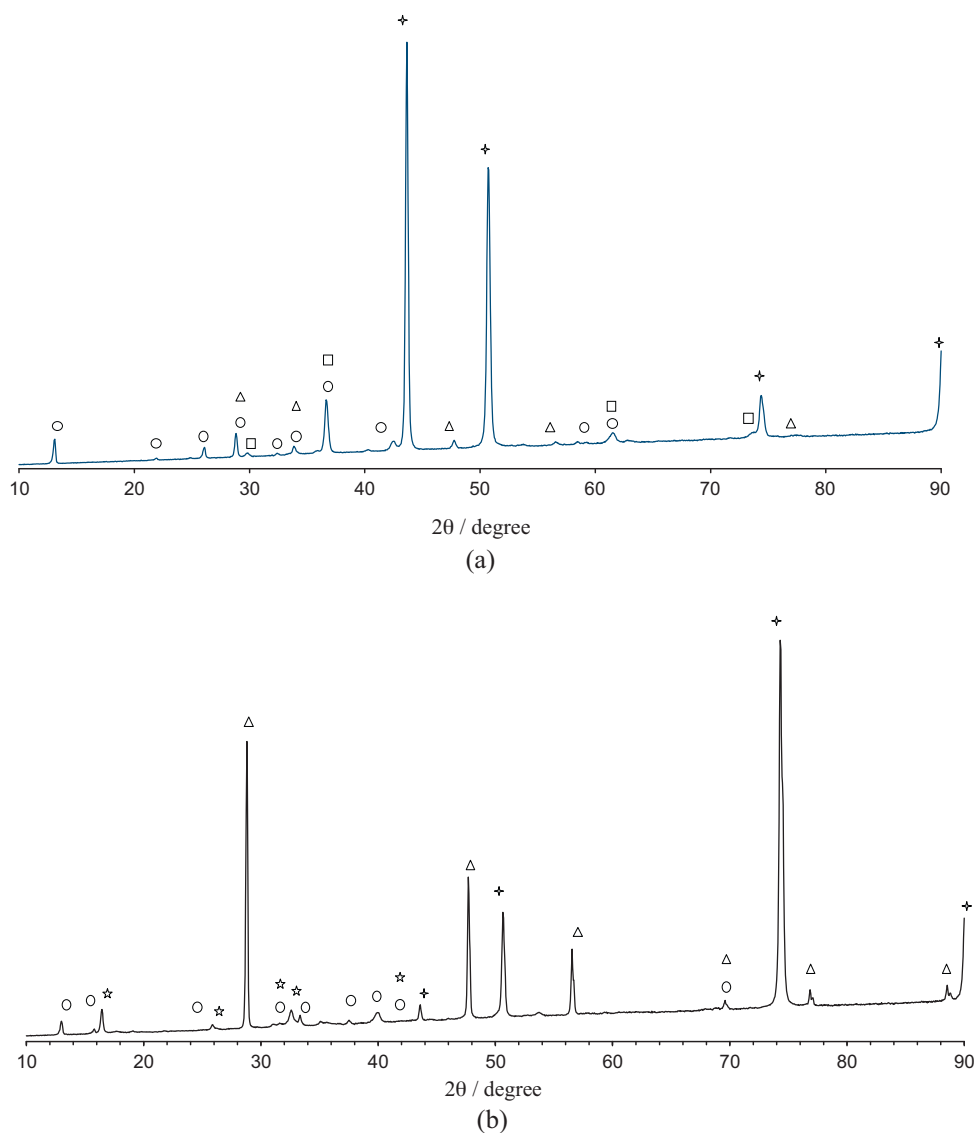
Fig. 11. XRD spectra of a copper sample coated with S1 (a) and S2 (b) patina. ○ Cu(NO₃)(OH)₃, △ CuCl, □ Cu₂O, ✦ Cu, ☆ Cu₂Cl(OH)₃.

successive immersion periods, contributing to localized corrosion activity within the pores (earlier pores development) and faster patina consolidation during drying periods. Another reason that can also contribute to the faster increase of the impedance response of the samples coated with patina S2 is the presence of the secondary pores (see discussion related to Fig. 5(d)), which would be more easily blocked by corrosion products, contributing to impedance increase.

The analysis of Fig. 10(c) demonstrates that after longer drying periods a protective corrosion product layer also precipitates in the pore walls of the sample intermittently exposed to the synthetic rainwater of São Paulo contributing to impedance increase, moreover as the HF loop is more depressed than that exhibited in Fig. 10(b), it is likely that a stronger contribution of secondary pores is present. In the diagram depicted in Fig. 10(c), in the LF region, a clear Warburg response develops indicating that the LF process must be different from that verified in the samples tested in the NaCl $0.1\,mol\,dm^{-3}$ solution. We propose that, as verified by Feng et al. [36] for copper corrosion in solutions with similar pH, the diffusion of copper ions through the oxide layer would be the rate limiting step, since cuprite must be the main component of the corrosion product layer formed in this solution [35]. The

cuprite precipitated in the pore walls would be responsible for the depressed HF capacitive loop.

Comparing the diagrams presented in Fig. 9 with those shown in Figs. 7 and 8, it is clear that impedance starts to increase earlier and that the HF capacitive loop develops sooner in the former figure. This indicates that the formation of the protective corrosion product layer within the pores takes less time in the intermittent tests performed in the synthetic rainwater of São Paulo. This can be likely due to a partial dissolution of the patina layer (see discussion related to Fig. 6) and to the lower aggressiveness of this solution, which contains fewer amounts of ionic species, particularly chloride ions, leading to higher stability of the corrosion product layer.

Fig. 12 shows the Nyquist diagram for the copper sample coated with patina S1 and intermittently exposed to the São Paulo synthetic rainwater solution during 28 days, corresponding to 4 immersion periods. Comparing this diagram with the one presented in Fig. 10(c) (corresponding to 3 immersion periods) it is verified that the HF loop is even flatter, demonstrating increasing contribution of secondary pores, and that the LF one makes an angle of approximately 22.5° with the real axis, which, according to de Levie [22], is characteristic of a diffusion controlled process within a pore with semi-infinite length. As a diagnosis test this

Table 3
Impedance modulus times the fourth root of the frequency for the higher frequency points of the low frequency capacitive loop of Fig. 12. In the three last columns are shown the values found by de Levie for a diffusion controlled process within a porous electrode with semi-infinite pore length [22].

Experimental values (Fig. 12)			Values presented by de Levie for the redox couple ferri/ferrocyanide in 1×10^{-3} mol dm^{-3} KCl solution using a silver working electrode		
Frequency (f) (Hz)	Impedance modulus (Ω cm^2)	$|Z| \times \sqrt[4]{f}$	Frequency (f) (Hz)	Impedance modulus (Ω cm^2)	$|Z| \times \sqrt[4]{f}$
21.135	2.14×10^3	4.59×10^3	19.6	14.8	31.2
17.278	2.22×10^3	4.53×10^3	27.1	13.5	30.8
14.125	2.34×10^3	4.54×10^3	39.4	12.3	30.7
11.548	2.46×10^3	4.53×10^3	56.9	11.1	30.6
9.4407	2.59×10^3	4.54×10^3	79.7	10.2	30.4
7.718	2.75×10^3	4.58×10^3	117	9.1	29.8
6.3096	2.91×10^3	4.61×10^3	250	7.5	29.8
5.1582	3.12×10^3	4.70×10^3	503	6.2	29.3
4.2169	3.25×10^3	4.66×10^3	1004	5.1	28.7
3.4475	3.54×10^3	4.82×10^3			
2.8184	3.40×10^3	4.40×10^3			
2.3041	3.89×10^3	4.79×10^3			
1.8836	4.12×10^3	4.83×10^3			
1.5399	4.33×10^3	4.82×10^3			
1.2589	4.73×10^3	5.01×10^3			
1.0292	4.97×10^3	5.00×10^3			

author [22] showed that when such process takes place the product between the impedance modulus and the fourth root of the frequency should be constant. Table 3 presents the results of such product for the higher frequency region of the LF loop of Fig. 12, the last three columns present the values found by de Levie in his work [22]. The values found from our experimental data are fairly constant indicating that a diffusion controlled process is taking place within the pores with semi-infinite pore length. Therefore, for this sample, after 28 days of test (4 immersion periods) a porous electrode with semi-infinite pore length is completely developed in the investigated frequency range.

A response similar to that presented in Fig. 12 was found by Frateur et al. [31] for the cast iron/drinking water system. These authors have interpreted their response as being due to a porous electrode which pores were coated by a compact microporous layer made up of green rust and calcium carbonates. In the present work we propose that the semi-infinite pores are coated by a cuprite layer (main corrosion product formed when copper is immersed in

Fig. 12. Nyquist diagram for copper electrode coated with S1 patina and intermittently exposed to the synthetic rainwater of São Paulo (28 days – 4 exposure periods). In the diagram the slopes of the straight line between the capacitive loops and the real axis are represented.
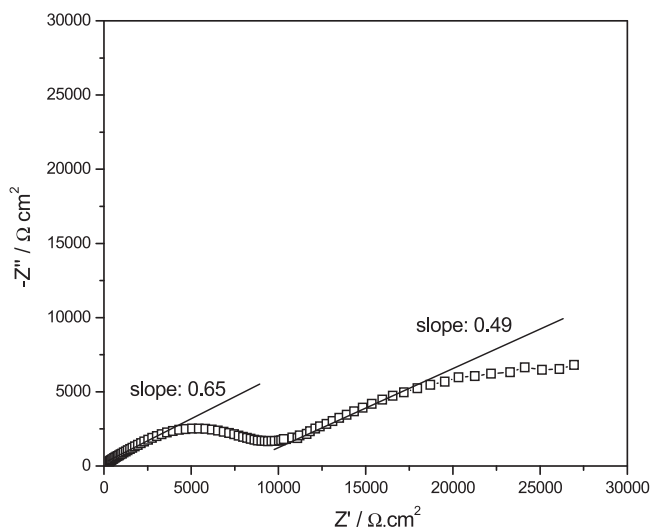
synthetic rainwater of São Paulo [35]) and that diffusion of copper ions through this layer [36] is responsible for the LF loop.

In all the intermittent exposure experiments, after a number of tests (5 in the 0.1 mol dm^{-3} NaCl solution, Figs. 7 and 8, and 4 in the synthetic rainwater of São Paulo, Fig. 9), two highly deformed capacitive loops were completely developed, which origins had already been discussed. This shape of diagram is similar to those obtained by other authors that used EIS to investigate the electrochemical behaviour of copper and bronze samples coated with natural or artificial patinas formed either during continuous exposure to different atmospheres [2,5,7] or under intermittent exposure conditions [2].

De Oliveira et al. [2] interpreted their EIS results as being due to the presence of a patina layer with porous structure on the top of their samples (the authors ascribed the depressed HF capacitive loop to this layer). On the other hand, Leygraf and co-workers [5,7] interpreted the two capacitive loops of their EIS diagrams as being representative of a bi-layered structure of the patinas. In one of the papers the authors used an equivalent circuit containing a series of two sub-circuits with parallel R//CPE [5] and in the other a cascade arrangement [7], containing the same elements, to fit the experimental data. In both cases [5,7] each capacitive loop was ascribed to one of the layers of the patina film.

In one of the papers of Leygraf [5] typical values of the patina layers thicknesses were given (cf. Table 1 [5]), which ranged from several units to few hundred micra, depending on the patina origin. The capacity of corrosion product layers with such thicknesses is incompatible with the frequency range and impedance values typically exhibited in the EIS diagrams of patinated copper samples, including those presented by Leygraf and co-workers [5]. Therefore, based on this reasoning the interpretation of the impedance results for patinated copper samples [2,5,7] can be classified as wrong and indeed the EIS experiments do not "see" the thick porous patina layer, as it does for coated metals. As an additional remark it must be pointed out that polarization resistance values obtained by Leygraf and co-workers [5] from their impedance diagrams were highly coherent with those calculated from polarization curves, further indicating that their EIS responses were related to the corrosion processes taking place at the substrate instead of being representative of the patina layer properties.

The discussion presented in the present work together with the comparison with other experimental EIS results available in the

Fig. 13. Physical model of the pores.

Fig. 14. Schematic representation of the sequence of events leading to the EIS response of the patina coated samples during wetting-drying cycles (intermittent tests): (a) rough electrode (flat electrode EIS response); (b) porous electrode with finite pore length (mixed porous-flat electrode EIS response); (c) porous electrode with semi-infinite pore.
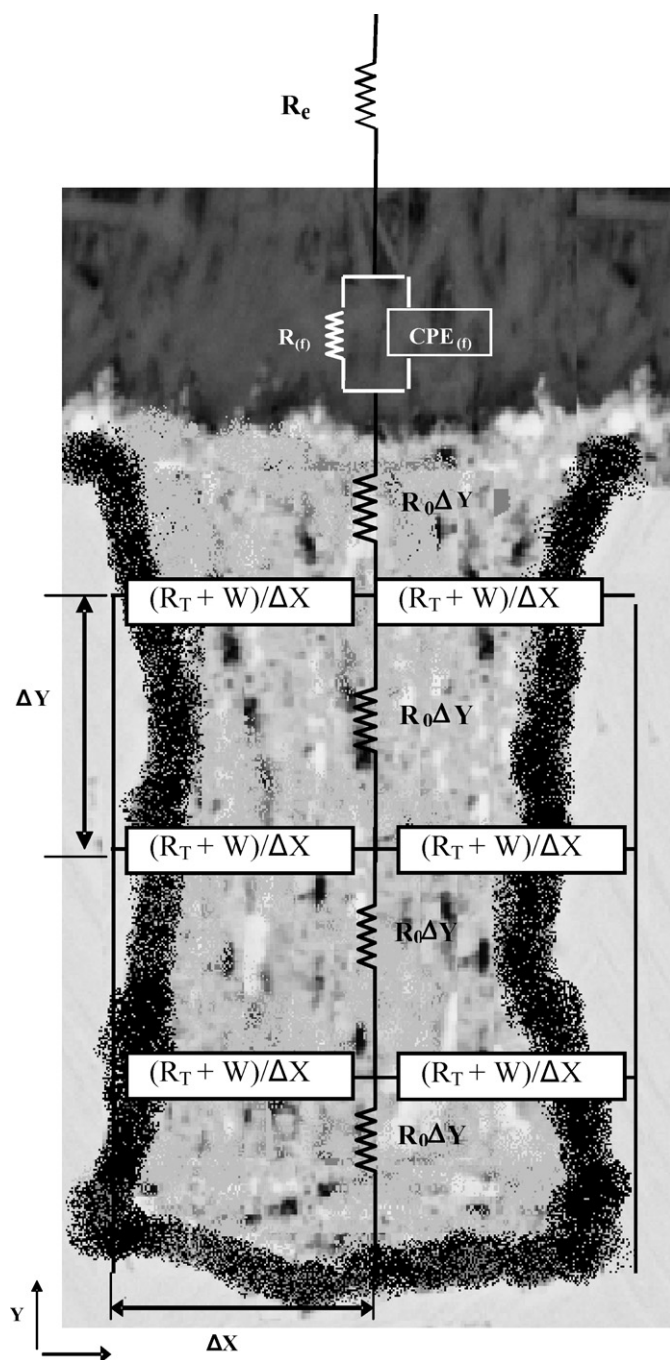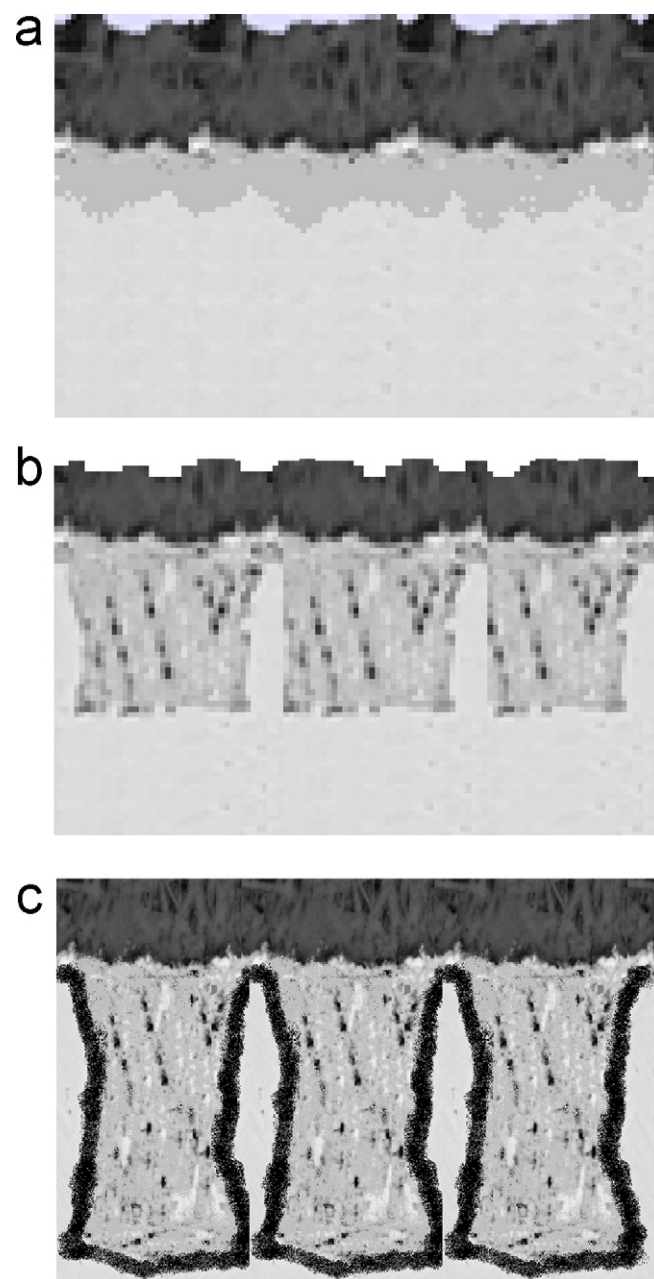
literature [2,5,7] indicate that, after consolidation, patina layers on copper and bronze exhibit porous electrode response irrespectively to their origin (either naturally or artificially produced) and age (some of the natural patinas examined in the works of Leygraf et al. [5,7] had more than one hundred years). Therefore a general physical model, represented in Fig. 13, can be proposed as being representative of the EIS response of patina layers formed on copper and bronze. In the model the patina layer itself is not detected by the EIS measurements, instead mainly the activity within the pores is detected. The results obtained in the present work also show that the nature of the electrolyte is determinant to pore development. In this way, when copper is exposed to an aggressive electrolyte (like NaCl 0.1 mol dm^{-3}) increasing in the pore length takes longer time, likely due to the maintenance of an intense electrochemical activ-

ity at the whole electrode surface. On the other hand, when less aggressive electrolytes are employed (like the São Paulo synthetic rainwater) the electrochemical activity is concentrated within the pores and an EIS response of porous electrode with semi-infinite pore length is developed earlier.

Fig. 14 presents schematically the proposed sequence of events taking place at the electrode surface due to patina aging during wetting and drying cycles. After patina production (Fig. 14(a)) the electrode surface becomes rough due to increased attack of the surface. During drying periods, pores would become deeper due to increasing electrochemical activity inside these cavities and a mixed porous-flat electrode response would be achieved in the EIS experiments (Fig. 14(b)). Finally, when sufficient wetting-drying cycles have occurred, the pores become deep enough and

a porous electrode response is obtained in the whole frequency range (Fig. 14(c)). In the present case EIS experiments detected the precipitation of corrosion products inside the pores, however, in some other cases it is possible that precipitation of this layer would not occur.

5. Conclusions

In the present work the EIS response of copper electrodes coated with two different artificial patinas and immersed either in 0.1 mol dm^{-3} NaCl or in synthetic rainwater of São Paulo was investigated by total and intermittent immersion tests. The results of the total immersion tests in both solutions showed that the patinas do not protect the substrate and that the corrosion mechanisms are similar to those exhibited by pure copper. Nevertheless, for the samples tested in the chloride containing solution, the EIS behaviour was ascribed to a porous electrode with finite pore length, which was related to the extreme etching of the substrate during the patina production procedure.

On the other hand, the results of the EIS experiments performed during the intermittent tests showed, for both patinas and for both solutions, the progressive development of a porous electrode response, where pore depth is dependent of the composition of the solution. Moreover, the results indicated the precipitation of a protective corrosion product layer on the pore walls during drying periods, contributing to improved anticorrosion properties.

The results of the present study together with other available in the literature for similar systems suggest that the porous electrode model can be assumed as general for aged patinas formed on copper either naturally or artificially.

Acknowledgement

References

[1] M. Watanabe, E. Toyoda, T. Handa, T. Ichino, N. Kuwaki, Y. Higashi, T. Tanaka, Corros. Sci. 49 (2007) 766.
[2] F.J.R. de Oliveira, D.C.B. Lago, L.F. Senna, L.R.M. de Miranda, E. D'Elia, Mat. Chem. Phys. 115 (2009) 761.
[3] L. Nuñez, E. Reguera, F. Corvo, E. Gonzalez, C. Vazquez, Corros. Sci. 47 (2005) 461.
[4] C. Chiavari, K. Rahmouni, H. Takenouti, S. Joiret, P. Vermaut, L. Robbiola, Electrochim. Acta 52 (2007) 7760.
[5] X. Zhang, W. He, I. Odnevall Wallinder, J. Pan, C. Leygraf, Corros. Sci. 44 (2002) 2131.
[6] L. Robbiola, R. Portier, J. Cult. Herit. 7 (2006) 1.
[7] J. Sandberg, I. Odnevall Wallinder, C. Leygraf, N. Le Bozec, Corros. Sci. 48 (2006) 4316.
[8] L. Robbiola, J.M. Blengino, C. Fiaud, Corros. Sci. 39 (1998) 2083.
[9] N. Souissi, L. Bousselmi, S. Khosrof, E. Triki, Mat. Corros. 57 (2006) 794.
[10] L. Muresan, S. Varvara, E. Stupnisek-Lisac, H. Otmacic, K. Marusic, S. Horvat-Kurbegovic, L. Robbiola, K. Rahmouni, H. Takenouti, Electrochim. Acta 52 (2007) 7770.
[11] I. Constantinides, A. Adriaens, F. Adams, Appl. Surf. Sci. 189 (2002) 90.
[12] J. Vilche, F. Varela, G. Acuña, E. Codaro, B.M. Rosales, A. Fernadez, G. Moriena, Corros. Sci. 39 (1997) 655.
[13] B. Rosales, R. Vera, G. Moriena, Corros. Sci. 30 (1999) 625.
[14] V. Costa, A. Texier, Communication at the International Conference on the Corrosion Conservation and Study of Historic Metals In Situ, Hildesheim, Germany, 2001.
[15] T.F.M. Leal, A.P.G. Fontele, J.J. Pedrotti, A. Fornaro, Quím. Nova 27 (2004) 855.
[16] R.P. Bendezú, H.R.P. Gonçalves, A.C. Neiva, H.G. de Melo, J. Braz. Chem. Soc. 18 (2007) 54.
[17] M.E. Orazem, N. Pébère, B. Tribollet, J. Electrochem. Soc. 153 (2006) B129.
[18] K. Nassau, A.E. Miller, T.E. Graedel, Corros. Sci. 27 (1987) 703.
[19] C. Deslouis, B. Tribollet, G. Mengoli, M.M. Musiani, J. Appl. Electrochem. 18 (1988) 374.
[20] C. Deslouis, B. Tribollet, G. Mengoli, M.M. Musiani, J. Appl. Electrochem. 18 (1988) 384.
[21] R. de Levie, Electrochim. Acta 8 (1963) 751.
[22] R. de Levie, Electrochim. Acta 9 (1964) 1231.
[23] R. de Levie, Electrochemical response of porous and rough electrodes, in: P. Delahay (Ed.), Advances in Electrochemistry and Electrochemical Engineering, vol. 6, Interscience New York, New York, 1967.
[24] A. Lasia, J. Electroanal. Chem. 397 (1995) 27.
[25] J.-P. Candy, P. Fouilloux, M. Keddam, H. Takenouti, Electrochim. Acta 26 (1981) 1029.
[26] J.-P. Candy, P. Fouilloux, M. Keddam, H. Takenouti, Electrochim. Acta 27 (1982) 1585.
[27] O.E. Barcia, E. D'Elia, I. Frateur, O.R. Mattos, N. Pébère, B. Tribollet, Electrochim. Acta 47 (2002) 2109.
[28] H.-K. Song, Y.-H. Jung, K.-H. Lee, L.H. Dão, Electrochim. Acta 44 (1999) 3513.
[29] J.-P. Diard, J.-M. Le Canut, B. Le Gorrec, C. Montella, Electrochim. Acta 16–17 (1998) 2485.
[30] J.B. Matos, E. D'Elia, O.E. Barcia, O.R. Mattos, N. Pébère, B. Tribollet, Electrochim. Acta 46 (2001) 1377.
[31] I. Frateur, C. Deslouis, M.E. Orazem, B. Tribollet, Electrochim. Acta 44 (1999) 4345.
[32] P.H. Suegama, V.H.V. Sarmento, M.F. Montemor, A.V. Benedetti, H.G. de Melo, I.V. Aoki, C.V. Santilli, Electrochim. Acta 55 (2010) 5100.
[33] Y. Gourbeyre, B. Tribollet, C. Dagbert, L. Hyspecka, J. Electrochem. Soc. 5 (2006) B162.
[34] D.A. Robinson, J.D. Cooper, C.M.K. Gardner, J. Hydrol. 255 (2002) 39.
[35] R.P.B. Hernández, Z. Pászti, H.G. de Melo, I.V. Aoki, Corros. Sci. 52 (2010) 826.
[36] Y. Feng, W.-K. Teo, K.-S. Siow, A.-K. Hsieh, Corros. Sci. 38 (1996) 387.
[37] U.R. Evans, Trans. Faraday Soc. 19 (1923) 201.